



TGF- β 1 attenuates mitochondrial bioenergetics in pulmonary arterial endothelial cells via the disruption of carnitine homeostasis

Xutong Sun^a, Qing Lu^a, Manivannan Yegambaram^a, Sanjiv Kumar^b, Ning Qu^a, Anup Srivastava^a, Ting Wang^c, Jeffrey R. Fineman^c, Stephen M. Black^{a,*}

^a Department of Medicine, Arizona Health Sciences Center, University of Arizona, Tucson, AZ, 85721, USA

^b Center for Blood Disorders, Medical College of Georgia at Augusta University, Augusta, GA, 30912, USA

^c Department of Internal Medicine University of Arizona, Phoenix, AZ, 85004, The Department of Pediatrics and the Cardiovascular Research Institute, University of California San Francisco, San Francisco, CA, 94143, USA



ARTICLE INFO

Keywords:

Mitochondrial bioenergetics
TGF- β 1
PPAR γ
ROS
NADPH oxidase
Mechanical forces

ABSTRACT

Transforming growth factor beta-1 (TGF- β 1) signaling is increased and mitochondrial function is decreased in multiple models of pulmonary hypertension (PH) including lambs with increased pulmonary blood flow (PBF) and pressure (Shunt). However, the potential link between TGF- β 1 and the loss of mitochondrial function has not been investigated and was the focus of our investigations. Our data indicate that exposure of pulmonary arterial endothelial cells (PAEC) to TGF- β 1 disrupted mitochondrial function as determined by enhanced mitochondrial ROS generation, decreased mitochondrial membrane potential, and disrupted mitochondrial bioenergetics. These events resulted in a decrease in cellular ATP levels, decreased hsp90/eNOS interactions and attenuated shear-mediated NO release. TGF- β 1 induced mitochondrial dysfunction was linked to a nitration-mediated activation of Akt1 and the subsequent mitochondrial translocation of endothelial NO synthase (eNOS) resulting in the nitration of carnitine acetyl transferase (CrAT) and the disruption of carnitine homeostasis. The increase in Akt1 nitration correlated with increased NADPH oxidase activity associated with increased levels of p47^{phox}, p67^{phox}, and Rac1. The increase in NADPH oxidase was associated with a decrease in peroxisome proliferator-activated receptor type gamma (PPAR γ) and the PPAR γ antagonist, GW9662, was able to mimic the disruptive effect of TGF- β 1 on mitochondrial bioenergetics. Together, our studies reveal for the first time, that TGF- β 1 can disrupt mitochondrial function through the disruption of cellular carnitine homeostasis and suggest that stimulating carnitine homeostasis may be an avenue to treat pulmonary vascular disease.

1. Introduction

Transforming Growth Factor- β 1 (TGF- β 1), a member of a superfamily that contains a group of diverse polypeptide responsible for multi cellular activities including proliferation and differentiation [1]. Endothelial cells respond to TGF- β 1 by their interaction with transmembrane serine/threonine kinase receptors and then propagate the signal to the nucleus via Smad signaling [2]. Prior work has shown that TGF- β signaling is intimately involved in the development of pulmonary hypertension (PH) although the roles of the ligands and receptors in the TGF- β family are still not well understood [3]. The presence of different TGF- β isoforms in the pulmonary vascular wall in the context of tissue remodeling in PH was initially identified by Botney et al in 1994 [4] and high levels of TGF- β 1 have been identified in EC and the interstitium of the plexiform lesions in advanced forms of PH

[5,6]. We have previously shown that the expression of TGF- β 1 and its receptors is increased in the endothelium of actively remodeling pulmonary vessels in lamb model of PH associated with increased pulmonary blood flow (PBF) and pressure [7]. The exposure of the pulmonary circulation to these abnormal mechanical insults results in progressive adaptive structural and functional abnormalities in the pulmonary vasculature [8–17]. Advanced structural changes are irreversible, but surgical correction can reverse early changes, which is the basis for the neonatal repair of these types of congenital heart defects [18]. Functional changes are not as readily addressed and even children with reversible disease suffer significant morbidity and mortality in the peri-operative period due to increased pulmonary vascular reactivity [8,19–24]. This can lead to severe hypoxemia, acidosis, low cardiac output, and death. Despite the clinical need, the precise mechanisms responsible for these aberrations pulmonary vascular reactivity remain

* Corresponding author. Division of Translational and Regenerative Medicine, Department of Medicine, The University of Arizona, Tucson, AZ, 85724, USA.
E-mail address: steveblack@email.arizona.edu (S.M. Black).

<https://doi.org/10.1016/j.redox.2020.101593>

Received 27 April 2020; Received in revised form 19 May 2020; Accepted 21 May 2020

Available online 31 May 2020

2213-2317/ © 2020 The Authors. Published by Elsevier B.V. This is an open access article under the CC BY-NC-ND license (<http://creativecommons.org/licenses/by-nc-nd/4.0/>).

unclear. Increasing evidence indicates that mitochondrial dysfunction is an important contributor to the development of PH [25,26]. Our recent studies indicate that mitochondrial dysfunction occurs secondary to disruptions in carnitine homeostasis and β -oxidation in children born with complex congenital heart defects that result in increased PBF [27–30]. However, the potential role of TGF- β 1 in the disruption of mitochondrial bioenergetics has not been resolved.

Our previous studies indicate that in our lamb model with increased PBF, the disruption of carnitine homeostasis correlates with a decrease in the protein levels of peroxisome proliferator-activated receptor gamma (PPAR γ) [29], a ligand-activated transcription factor belonging to the nuclear hormone receptor family. PPAR γ is abundantly expressed in vascular tissues [31], and its deficiency is associated with PH [32]. Further, our previous studies have shown that PPAR γ is an important regulator of fatty acid oxidation (FAO) [29]. Thus, the purpose of this study was to determine whether there was a link between elevated TGF- β 1 levels, carnitine homeostasis, and the development of mitochondrial dysfunction and to evaluate the role played by PPAR γ signaling. Our data, obtained in PAEC, indicate that TGF- β 1 disrupts both carnitine homeostasis and mitochondrial bioenergetics. The disruption of carnitine homeostasis correlated with an increase the nitration of CrAT secondary to Akt-1 mediated mitochondrial redistribution of eNOS. Further, we found that the Akt1 activation caused by its nitration is due to a loss of PPAR γ activity and an increase in NADPH oxidase activity.

2. Materials and methods

2.1. Antibodies and chemicals

Antibodies against PPAR- γ , Akt1, phospho-Akt at Ser473 and VDAC were purchased from Cell Signaling (Danvers, MA). Antibodies against eNOS, p67^{phox}, and p47^{phox} were purchased from BD Transduction laboratories (San Jose, CA). The anti-Rac1 and anti-phospho S617-eNOS were purchased from EMD Millipore (Temecula, CA). The anti-nitrotyrosine antibody was obtained from EMD Millipore (Billerica, MA). The anti-3-Nitrotyrosine antibody (cat#:ab110282) was obtained from Abcam (Cambridge, MA). The anti-CrAT was obtained from Proteintech (Rosemont, IL). The nitro-Tyr³⁵⁰ Akt1-specific antibody was raised against a synthetic peptide antigen CGRLPF(Y-NO₂)NQDHEKL, where Y-NO₂ represents 3-nitrotyrosine as described [33]. Antibody against β -actin, TGF- β 1 and GW9662 were purchased from Sigma (St. Louis, MO). MitoTracker (cat#: M22425) and Tetramethylrhodamine (TMRM) were obtained from Invitrogen (Carlsbad, CA).

2.2. Cell culture and treatment

Primary cultures of ovine PAEC were isolated and cultured as described previously [34]. Briefly, cells were isolated by the explant technique. The heart and lungs were obtained from fetal (138–140d gestation) lambs after death. These fetal lambs had not undergone previous surgery or study. The main and branching pulmonary arteries were removed and the exterior of the vessel was rinsed with 70% ethanol. The vessel was opened longitudinally, and the interior was rinsed with PBS to remove blood. The endothelium was lightly scraped away, placed in medium DME-H16 (with 10% fetal bovine serum and antibiotics), and incubated at 37 °C in 21% O₂–5% CO₂–balance N₂. After 5d, islands of endothelial cells were cloned to ensure purity. When confluent, the cells were passaged to maintain them in culture or frozen in liquid nitrogen. Endothelial cell identity was confirmed by the typical cobblestone appearance, contact inhibition, specific uptake of acetylated low-density lipoprotein labeled with 1,1'-dioctadecyl-3,3,3',3'-tetramethylindocarbocyanine Willebrand factor (Dako, Carpinteria, CA). Cells were used before passage 13. For TGF- β 1 treatment, standard medium was replaced with serum free medium for 8 h. For

GW9662 treatment, standard medium was replaced with 0.2% FBS medium for 24 h.

2.3. Western blot analysis

Total protein prepared from cells (20 μ g) were separated on 4–20% SDS-polyacrylamide gels and transferred to polyvinylidene difluoride membranes (PVDF). Immunoblotting was carried out using the appropriate antibodies in Tris-base buffered saline with 0.1% Tween 20 and 5% nonfat milk. After washing, the membranes were probed with horseradish peroxidase-conjugated goat antiserum to rabbit or mouse. Reactive bands were visualized using chemiluminescence (Super Signal West Femto; Pierce, Rockford, IL) on a LI-COR Odyssey image station (Lincoln, NE). Bands were quantified using LI-COR Image Station software. Loading was normalized by reprobing the membranes with an antibody specific to β -actin. To determine the levels of eNOS in mitochondria, mitochondrial protein extracts (5 μ g) were separated on 4–20% SDS-PAGE and transferred to PVDF. Immunoblotting was carried out using the eNOS antibody in Tris-base buffered saline with 0.1% Tween 20 and 5% nonfat milk. Loading was normalized by reprobing the membranes with the mitochondrial marker voltage-dependent anion channel (VDAC).

2.4. Immunoprecipitation analysis

The interactions of eNOS/hsp90 levels were analyzed by immunoprecipitation analysis as described [35]. The efficiency of immunoprecipitation was normalized by reprobing the membranes with the immunoprecipitation antibody (IB:eNOS). For nitrated CrAT, PAEC were washed twice in ice-cold PBS and incubated on ice for 30 min in lysis buffer containing 1% NP40, 20 mM Tris-HCl (pH 7.5), 137 mM NaCl, and protease inhibitor cocktail (Pierce, Rockford, IL). Cell lysates were then clarified by centrifugation at 20,000 g (20 min at 4 °C), the protein concentrations were determined, and 1 mg of each lysate was incubated overnight at 4 °C with a mouse antibody against 3-Nitrotyrosine (6 μ g; Abcam, Cambridge, MA) in 1-ml final volume at 4 °C overnight. Protein G plus/protein A agarose (40 μ l; Calbiochem, Gibbstown, NJ) was added and rotated at 4 °C for an additional 2 h. The immune complexes were precipitated by centrifugation, washed three times with lysis buffer, boiled in SDS sample buffer, and subjected to SDS-PAGE gel. Nitrated CrAT protein levels were then detected using Western blot analysis.

2.5. Mitochondrial isolation

The mitochondria were isolated using Pierce Mitochondria isolation kits (Pierce, Rockford, IL) according to the manufacturer's guidelines as previously described [36,37].

2.6. Determination of ATP levels

ATP levels were estimated by using a Colorimetric/Fluorometric ATP Assay Kit (BioVision, Milpitas, CA) following the manufacturer's instructions. Briefly, cultured PAEC were treated with or without TGF- β 1 (5 ng/ml, 8 h). Cells were lysed and centrifuged at 13,500 rpm for 20 min. Deproteinize cell lysate by using Deproteinize Sample Preparation Kit (BioVision, Milpitas, CA). The supernatant of deproteinized cell lysate (50 μ L) was transferred to a 96-well plate, and then mixed with ATP detection working solution (50 μ L). The absorbance (OD570) was measured in a micro-plate reader (BioTek instruments Inc., Winooski, Vermont). The protein concentration of each group was also determined using a Pierce BCA Protein Assay Kit (Thermo scientific, Rockford, IL). The relative ATP level was represented as ATP value/protein value.

2.7. Measurement of NOX-derived superoxide levels

To detect superoxide generation, EPR measurements were performed using the spin trap, 1-Hydroxy-3-methoxycarbonyl-2,2,5,5-tetramethylpyrrolidine.HCl (CMH, 20 μ M in DPBS + 25 μ M desferrioxamine; Enzo Life Sciences, La Jolla, CA) as we have described [36,38]. NOX derived superoxide was measured by pre-incubating cells with the NADPH oxidase inhibitor, apocynin (100 μ M, Sigma-Aldrich) for 30 min followed by incubation with CMH. EPR spectra were analyzed using ANALYSIS v.2.02 software (Magnettech). Differences between samples incubated in the presence and absence of apocynin represented the level of NOX derived superoxide generation, reported as pmols/min/mg protein.

2.8. Measurement of NADPH oxidase activity

Measurement of NADPH oxidase activity was carried out as described previously [39]. Briefly, cells were trypsinized, pelleted, then homogenized with Tris-sucrose buffer (10 mM Tris base (Fisher, Pittsburgh, PA, USA), 340 mM sucrose (Mallinkrodt Baker, Phillipsburg, NJ, USA), 1 mM EDTA (Mallinkrodt Baker), 10 μ g/ml protease inhibitor mixture (Sigma)). The homogenate protein concentration was measured. NADPH oxidase activity was measured by a luminescence assay in the reaction buffer with 5 μ M lucigenin, 1 mM EGTA, and 50 mM phosphate buffer, pH 7.0. One hundred micrograms of homogenate protein + 100 μ M NADPH as substrate (Sigma) was added to an 8-mm test tube with 500 μ l reaction buffer and then incubated at 37 °C for 5 min. Photon emission was measured at 15 s in a luminometer (Model TD-20/20; Turner Designs, Sunnyvale, CA, USA).

2.9. Exposure of PAEC to laminar shear stress

Laminar shear stress was applied using a cone-plate viscometer that accepts six-well tissue culture plates, as described previously [40]. This method achieves laminar flow rates that represent physiological levels of laminar shear stress in human pulmonary arteries, which are approximately 20 dyn/cm² [41]. PAEC in the presence and absence of TGF- β 1 (5 ng/ml, 8 h) were acutely exposed or not to 20 dyn/cm² of shear stress for 15 min as described [42]. The media and cells were collected and used for further experiments.

2.10. Detection of NO_x

NO generated by PAEC in response to shear was measured using a NO-sensitive electrode with a 2-mm diameter tip (ISO-NOP sensor, WPI) connected to a NO meter (ISO-NO Mark II, WPI) as described previously [43].

2.11. Mitochondrial localization of eNOS

PAEC were transfected with a GFP tagged eNOS expression plasmid (eNOS-GFP) [44]. After 48 h transfection, cells were labeled with 100 nM MitoTracker (cat#: M22425, Invitrogen, Carlsbad, CA) for 30 min. This dye is not dependent on the mitochondrial membrane potential. The cells were then treated with TGF- β 1 (5 ng/ml, 8 h) or GW9662 (5 μ M, 24 h) and imaged using a fluorescence microscope (Applied Precision, Issaquah, WA, USA). Mitochondrial localization of eNOS was determined by calculating the Pearson product moment correlation coefficient [45] between images (green for eNOS-GFP and red for MitoTracker) using FITC (excitation 490nm/emission 528 nm) and TRITC (excitation 555nm/emission 617 nm). Magnification used was 60 \times .

2.12. Measurement of peroxynitrite levels

The level of cell peroxynitrite was determined by the oxidation of

dihydrorhodamine (DHR) 123 (EMD Millipore, Billerica, MA) to rhodamine 123, as we have described [46]. Briefly, cultured PAEC were treated with or without TGF- β 1 (5 ng/ml, 8 h) or GW9662 (5 μ M, 24 h). Collect the cells and cell pellet were then treated with PEG-Catalase (100U, 30min) to reduce H₂O₂ dependent DHR 123 oxidation. DHR 123 (5 μ mol/l, 30min) was added to the cell pellet in phenol red-free media and the fluorescence of rhodamine 123 measured using a Fluoroskan Ascent Microplate Fluorometer with excitation at 485 nm and emission at 545 nm. Fluorescent values were normalized to the protein levels in each sample.

2.13. Determination of mitochondrial ROS levels and mitochondrial membrane potential

MitoSOX™ Red mitochondrial ROS indicator (Molecular Probes, Grand Island, NY) a fluorogenic dye for detection of ROS in the mitochondria of live cells was used. Mitochondrial membrane potential was determined using TMRM (tetramethylrhodamine methyl ester perchlorate, Molecular Probes, Eugene, OR). Briefly, cells were washed with fresh media, incubated in media containing MitoSOX Red (5 μ M) or TMRM (50 nM), for 30 min at 37 °C in dark conditions, then subjected to fluorescence microscopy using an excitation of 510 nm and an emission at 580 nm (for MitoSOX) or an excitation of 548 nm and an emission at 575 nm (for TMRM). An Olympus IX51 microscope equipped with a CCD camera (Hamamatsu Photonics) was used for acquisition of fluorescent images. The average fluorescent intensities (to correct for differences in cell number) were quantified using ImagePro Plus version 5.0 imaging software (Media Cybernetics).

2.14. Analysis of mitochondrial bioenergetics

The XF24 Analyzer (Seahorse Biosciences, North Billerica, MA, USA) and XF Cell Mito Stress Test Kit (# 101706-100; Seahorse Biosciences) were used for the mitochondrial bioenergetic analyses. The optimum number of cells/well was determined to be 75,000/0.32 cm². Cells were exposed to TGF- β 1 (5 ng/ml, 8 h) or GW9662 (5 μ M, 24 h). The XF24 culture microplates were then incubated in a CO₂-free XF prep station at 37 °C for 45 min to allow temperature and pH calibration. For the Mito Stress test, we sequentially injected Oligomycin (1 μ M final concentration), carbonyl cyanide 4-(trifluoromethoxy) phenylhydrazone (FCCP, 1 μ M final concentration), and Rotenone + antimycin A (1 μ M final concentration of each) and measured the oxygen consumption rate (OCR). Using these agents, we determined basal mitochondrial respiration, reserve respiratory capacity and maximal respiratory capacity measurements in pmoles/min of oxygen consumed.

Respiratory chain complex I functional analysis in permeabilized pulmonary arterial endothelial cells.

This was carried out as previously described [47]. Briefly, PAEC were seeded in an XF24 cell culture microplate at 75,000 cells per well overnight. On the days of the experiment, cells were washed with 1 \times MAS buffer (Mannitol 220 mM, Sucrose 70 mM, KH₂PO₄ 10 mM, MgCl₂ 5 mM, HEPES 2 mM, EGTA 1 mM, Fatty Acid Free (FAF) BSA 0.2% (w/v)). A Pyruvate/Malate/ADP (10 mM/1 mM/4 mM respectively) mixture was added to the MAS buffer to form the assay medium. Prior to starting the assay, mitochondrial Complex I substrates and inhibitors, in 1 \times MAS buffer, were added to the injection ports of the cartridge: Port 1: Complex I inhibitor – rotenone (2 μ M). Cells were then treated with plasma membrane permeabilizer (1 nM XF PMP (Seahorse Biosciences), final volume of 0.5 ml per well) mixed with assay medium to initiate the experiment and immediately transferred to the XF24 analyzer. Initial readings were used to determine the basal OCR of respiring mitochondria (Stage 1). To determine the Complex I component of the OCR, the Complex I inhibitor, rotenone (2 μ M) was injected (Stage 2). The difference in OCR between Stage 1 and 2 was attributed to the respiratory activity of Complex I. In the assay we utilized mix/wait/measure times of 0.5 min/0.5 min/2 min with no

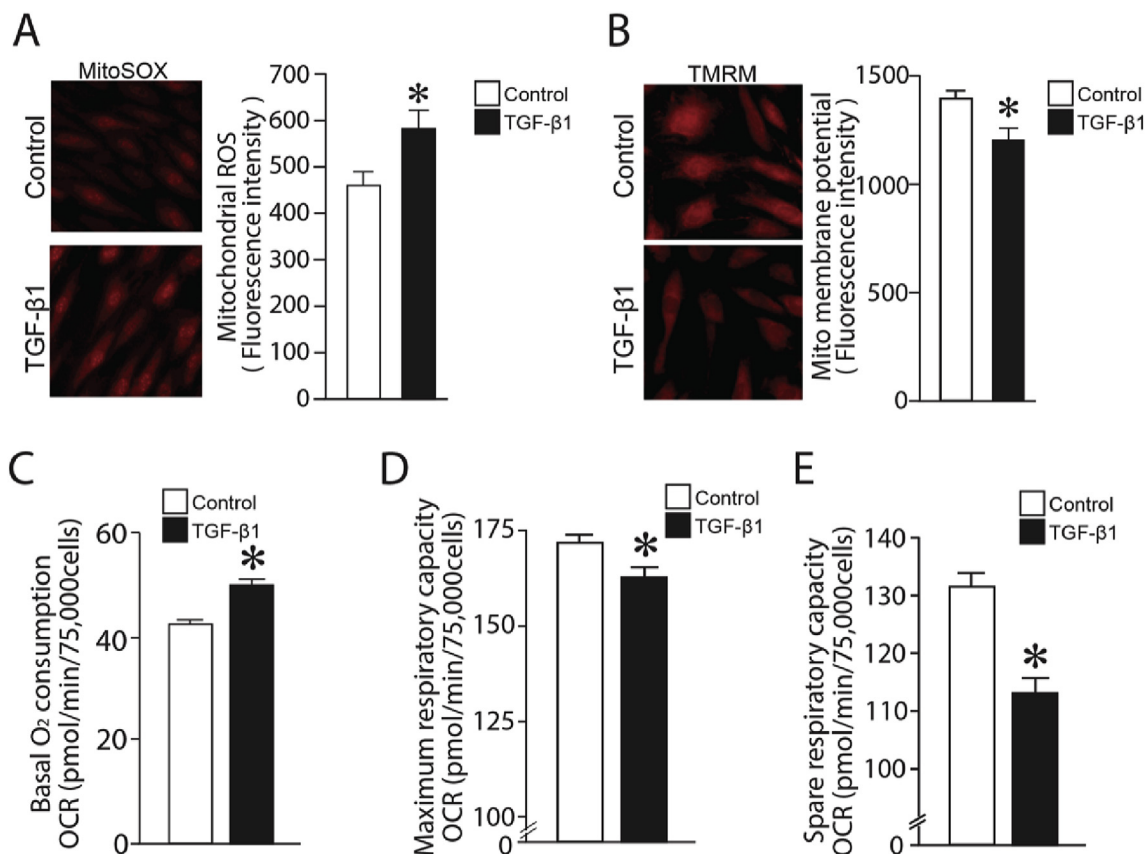


Fig. 1. TGF- β 1 induces mitochondrial dysfunction and mitochondrial bioenergetics disruption in pulmonary arterial endothelial cells. TGF- β 1 (5 ng/ml, 8 h) increases mitochondrial reactive oxygen species (ROS) generation in PAEC (A) and reduces the mitochondrial membrane potential (B). TGF- β 1 also affects mitochondrial bioenergetics as determined by significant increases in basal mitochondrial respiration (C) and reductions in the maximal respiratory capacity (D) and the spare respiratory capacity (E). Values are means \pm SEM; n = 6 (A&B). n = 22–24(C–E). *P < 0.05 vs. untreated.

equilibration step and took 2 measurements per step.

2.15. Fatty acid oxidation (FAO) assay

For the XF Palmitate-BSA Fatty Acid Oxidation (FAO) test, PAEC transfected with scrambled siRNA or CrAT siRNA (25 nM) were plated on XF24 culture microplates 75,000 cells/well the day before experiment. On the day of the assay, the cells were washed with freshly prepared FAO medium (KHB medium containing 2.5 mM glucose, 0.5 mM carnitine and 5 mM HEPES, pH7.4). FAO medium (412.5 μ l/well) was then added to each well and the plate incubated in a CO₂-free XF prep station at 37 °C for 40 min to allow temperature and pH calibration. The plates were then placed in the XF24 Analyzer and the OCR measured before injection (87.5 μ l/well) with BSA or Palmitate-BSA (Seahorse Bioscience, Part# 102720-100). The change in OCR was then determined.

Quantification of carnitine levels by high-performance liquid chromatography (HPLC).

Detection of carnitines was performed using an Agilent 1260 HPLC system with an Agilent 5 μ m C18 column (4.6 \times 150 mm) and equipped with a 1260 FLD fluorescence detector (Agilent Technologies, Inc.). Total and free carnitine levels were quantified by fluorescence detection at 248 nm (excitation) and 418 nm (emission). The acyl carnitines were calculated by subtracting the free carnitine values from the total carnitine values for all the samples as previously described [27].

2.16. Statistical analysis

Statistical analysis was performed using GraphPad Prism version

4.01 for Windows (GraphPad Software). The mean \pm SEM were calculated for all samples and significance was determined either by the unpaired *t*-test (for 2 groups) or ANOVA (for \geq 3 groups) with Newman-Keuls post-hoc testing. A value of *p* < 0.05 was considered significant.

3. Results

3.1. TGF- β 1 disrupts mitochondrial bioenergetics in PAEC by attenuating β -oxidation

Increased mitochondrial reactive oxygen species (ROS) generation [48] and disrupted mitochondrial membrane potential [48] are considered to be hallmarks of mitochondrial dysfunction. We determined the effect of TGF- β 1 on mitochondrial superoxide levels by measuring changes in MitoSOX red fluorescence. Our data indicated that exposure of cells to 5 ng/ml TGF- β 1 for 8 h caused a significant increase in MitoSOX fluorescence (Fig. 1A). Mitochondrial membrane potential was also decreased, as suggested by using TMRM fluorescence (Fig. 1B). Our previous studies have shown that mitochondrial function is linked to mitochondrial bioenergetics [36,37]. Using the Seahorse XF24 Analyzer, we next examined the effect of TGF- β 1 on mitochondrial bioenergetics in PAEC. Our data indicate that, although basal respiration was increased (Fig. 1C), both the maximal (Figure 1D) and spare (Figure 1E) respiratory capacities were significantly reduced by TGF- β 1. Further, we found that the disruption of mitochondrial bioenergetics correlated with reductions in complex I activity (Fig. 2A). We have previously demonstrated that mitochondrial bioenergetics can be attenuated secondarily to a disruption of carnitine homeostasis and the loss of FAO [27,29]. Our data demonstrate that carnitine homeostasis is reduced as determined by an increase in acyl-L-carnitine levels (Fig. 2B)

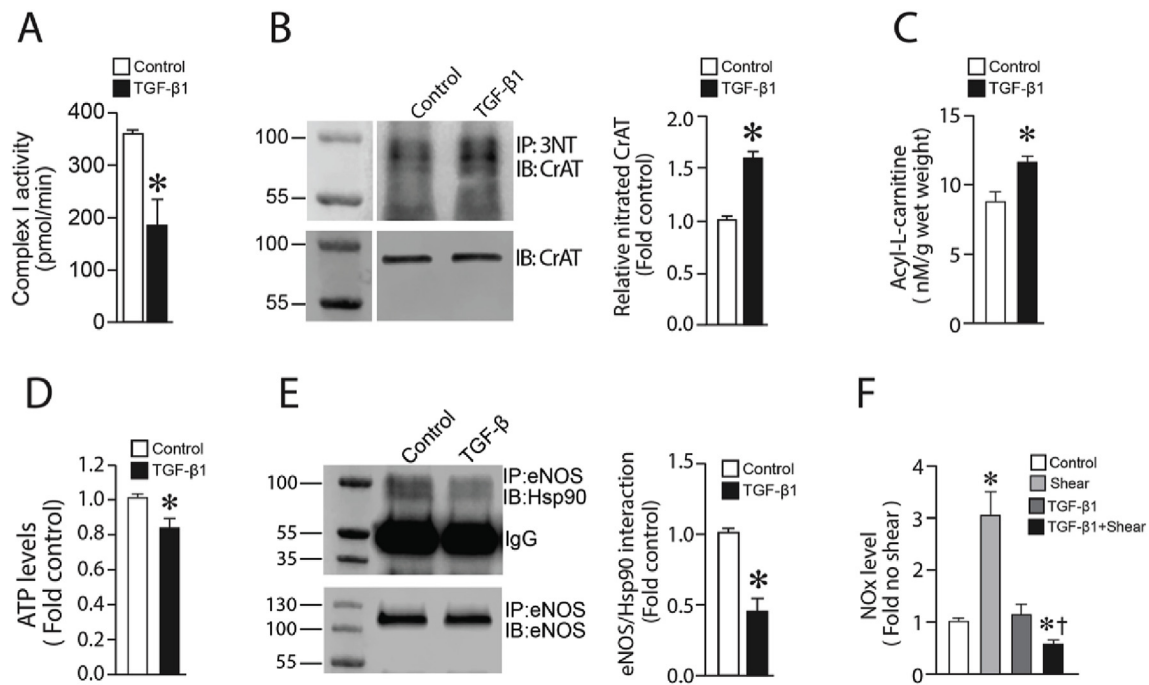


Fig. 2. TGF- β 1 disrupts carnitine homeostasis and NO signaling in pulmonary arterial endothelial cells. TGF- β 1 (5 ng/ml, 8 h) disrupts mitochondrial complex I activity (A) and this correlates with an increase in CrAT nitration, determined using IP/IB analysis (B) resulting in a disruption in carnitine homeostasis (C). Cellular ATP levels are significantly reduced (D) and the interaction of hsp90 with eNOS is decreased (E). TGF- β 1 also attenuates acute shear stress (20 dyn/cm², 15min)- increased NO generation. Values are means \pm SEM; n = 6–10. *P < 0.05 vs. untreated.

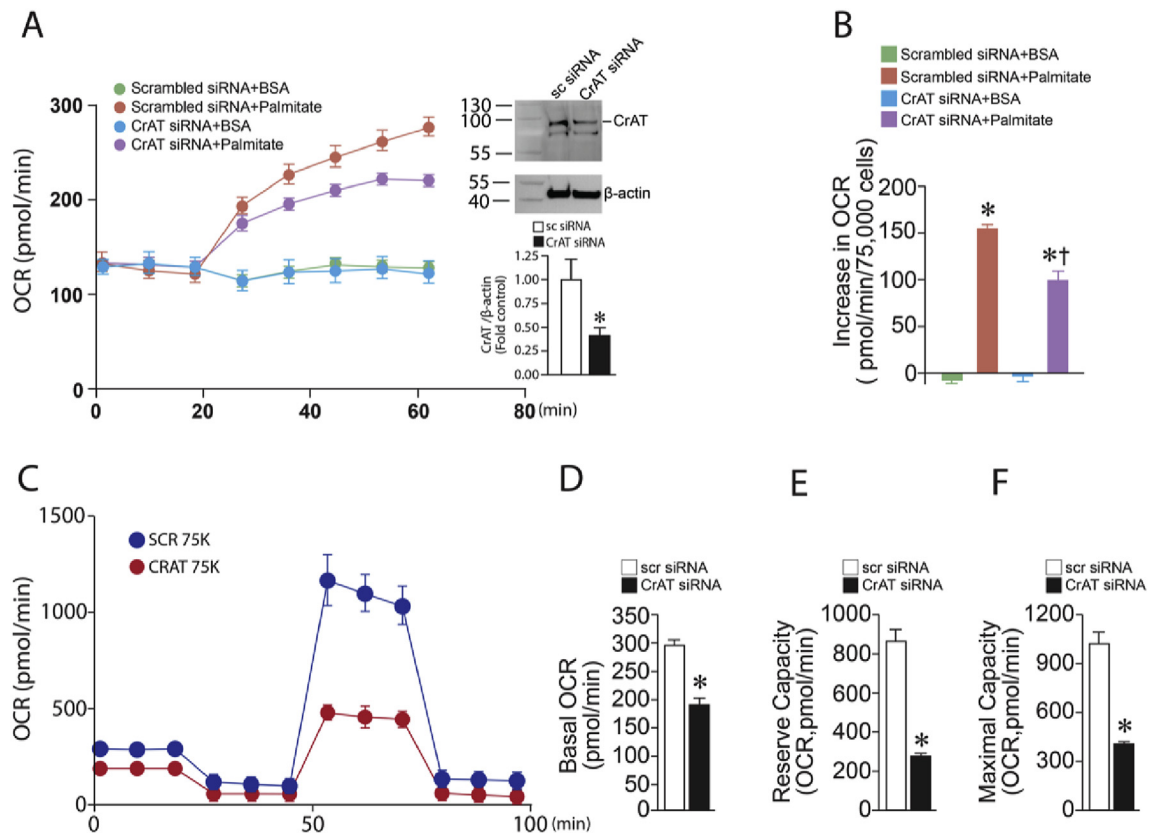


Fig. 3. Reducing carnitine acetyl transferase (CrAT) expression mimics the effect of TGF- β 1 on mitochondrial bioenergetics in pulmonary arterial endothelial cells. PAEC were transiently transfected with an siRNA to CrAT for 48 h to decreased CrAT expression (A, insert). Decreasing CrAT expression attenuates β -oxidation as demonstrated by a significant reduction in OCR after the injection of BSA-palmitate as substrate (A&B). Decreasing CrAT also significantly attenuates mitochondrial bioenergetics (C) as demonstrated by significant decreases in basal- (D), reserve- (E), and maximal (F)-respiratory capacity. Values are means \pm SEM; n = 5. *P < 0.05 vs. BSA alone (B) or scrambled siRNA (D–F); †P < 0.05 vs. scrambled siRNA + BSA palmitate (B).

and this is associated with the nitration of carnitine acetyl transferase (CrAT, Fig. 2C). We have previously shown that nitration inhibits CrAT activity [27]. In addition, we found that cellular ATP levels were reduced (Fig. 2D) and the activity of the ATP-dependent molecular chaperone, hsp90 was attenuated as determined by decreases in its interaction with eNOS (Fig. 2E). Furthermore, TGF- β 1 attenuated acute shear stress stimulated NO release (Fig. 2F). To confirm that the nitration-mediated loss of CrAT activity is involved in the loss of mitochondrial bioenergetics in PAEC we utilized an siRNA approach to decrease CrAT expression (Fig. 3A insert) and cellular FAO capacity (Fig. 3A and B). Decreasing FAO in cells mimicked the inhibitory effects of TGF- β 1 on mitochondrial bioenergetics (Fig. 3C) producing significant decreases in basal- (Fig. 3D), reserve- (Fig. 3E), and maximal (Fig. 3F)-respiratory capacity.

3.2. TGF- β 1 induces eNOS mitochondrial translocation in PAEC

Our previous studies have shown that the nitration of CrAT can occur due to the mitochondrial redistribution of eNOS [36] which is dependent on the Akt1-mediated phosphorylation of eNOS at S617 [49]. Thus, we next evaluated the effect of TGF- β 1 on eNOS mitochondrial translocation, eNOS phosphorylation and Akt1 activity. Our data indicate that TGF- β 1 significantly increased eNOS expression and mitochondrial localization (Fig. 4A&B). This was associated with increased eNOS phosphorylation at S617 (Fig. 4C) and Akt1 activity, as estimated by increased phosphorylation at S473 (Fig. 4D). We have shown that Akt1 activity can be stimulated via protein nitration [33,49] and our data confirmed that TGF- β 1 significantly increased peroxynitrite-dependent DHR123 oxidation levels (Fig. 4E), as well as Akt1 nitration (Fig. 4F). Taken together, these data demonstrate that TGF- β 1 induces eNOS mitochondrial translocation, ROS-mediated Akt1 activation, and eNOS phosphorylation at Ser617.

3.3. TGF- β 1 increases ROS levels by activating NADPH oxidase in PAEC

Peroxynitrite is formed by the interaction of NO with superoxide. NADPH oxidase (NOX) is a major contributor of ROS in cells of the vasculature during active metabolism [50]. Further, our prior studies have shown that TGF- β 1 can stimulate NOX activity and superoxide levels in pulmonary arterial smooth muscle cells [51]. Thus, we next determined if NOX was the source of the superoxide required for the formation of peroxynitrite and the nitration of Akt1. Our data demonstrate TGF- β 1 significantly increased the expression of the NOX subunit proteins p67^{phox} (Fig. 5A), p47^{phox} (Fig. 5B), and Rac1 (Fig. 5C) in PAEC. Furthermore, NOX activity (Fig. 5D) and NOX-derived superoxide (Fig. 5E) are both elevated by TGF- β 1 challenge, implicating NOX as the superoxide source required for Akt1 nitration and activation. Further we found that the increase in NOX activity correlated with a decrease in PPAR- γ protein levels (Fig. 5F). To confirm the role of PPAR- γ in the activation of NOX, we treated PAEC with the PPAR- γ antagonist GW9662 (5 μ M, 24 h). Our results demonstrate that GW9662 mimics the effects of TGF- β 1 treatment as demonstrated by decreases in PPAR- γ protein (Fig. 6A) and increases in p47^{phox} (Fig. 6B), p67^{phox} (Fig. 6C), and Rac1 (Fig. 6D) protein levels in PAEC. These changes in NOX protein subunits correlated with increases in NOX activity (Fig. 6E) and NOX-derived superoxide levels (Fig. 6F).

The PPAR- γ antagonist, GW9662 induces the mitochondrial translocation of eNOS in PAEC.

GW9662 treatment increased peroxynitrite levels (Fig. 7A) as well as Akt1 nitration (Fig. 7B) and activity, estimated via increases in pSer473Akt1 (Fig. 7C). GW9662 treatment also increased the levels of p617eNOS (Figure 7D) resulting in the mitochondrial redistribution of eNOS levels (Fig. 7E&F). GW9662 treatment also increased nitrated CrAT (Fig. 8A) resulting in an increase in acyl-L-carnitine levels (Fig. 8B). Mitochondrial function was also disrupted as determined by

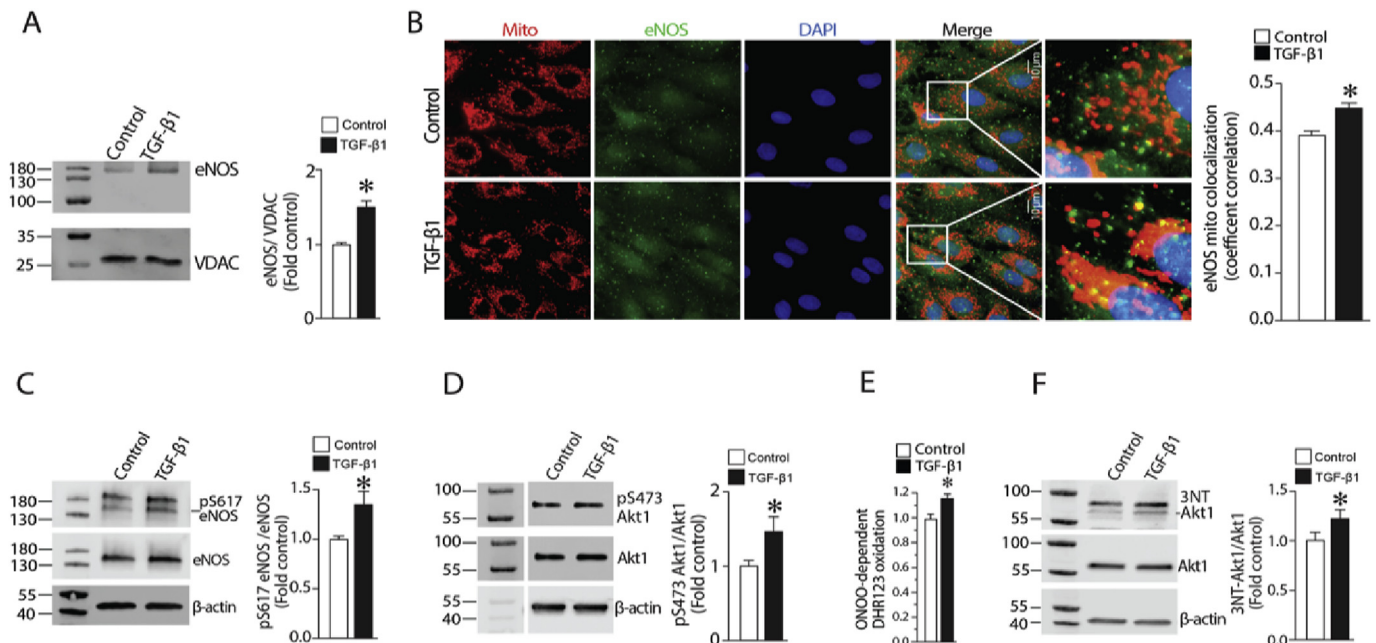


Fig. 4. TGF- β 1 induces the mitochondrial redistribution of eNOS in pulmonary arterial endothelial cells. PAEC were exposed to TGF- β 1 (5 ng/ml, 8 h) and the effect on the mitochondrial redistribution of eNOS determined. Mitochondrial protein extracts (5 μ g) were subjected to Western blotting using an antibody raised against eNOS. TGF- β 1 increases eNOS accumulation in the mitochondria (A). Loading was normalized by reprobing with the mitochondrial protein VDAC. PAEC were also transiently transfected with a GFP-tagged eNOS. The mitochondria were labeled with MitoTracker (red) and the cells were exposed or not to TGF- β 1. The extent of mitochondrial localization of eNOS was then determined by measuring the intensity of yellow fluorescence (overlap of red fluorescence of MitoTracker and green fluorescence of eNOS-GFP). There is an increase in yellow fluorescence in the TGF- β 1 treated cells (B). In addition, Western blotting demonstrated that TGF- β 1 significantly increased the phosphorylation of eNOS at S617 (C) and Akt1 at S473 (D). Peroxynitrite levels (E) and nitrated Akt1 (F) were also significantly increased. Values are means \pm SEM; n = 3–16. *P < 0.05 vs. untreated. (For interpretation of the references to colour in this figure legend, the reader is referred to the Web version of this article.)

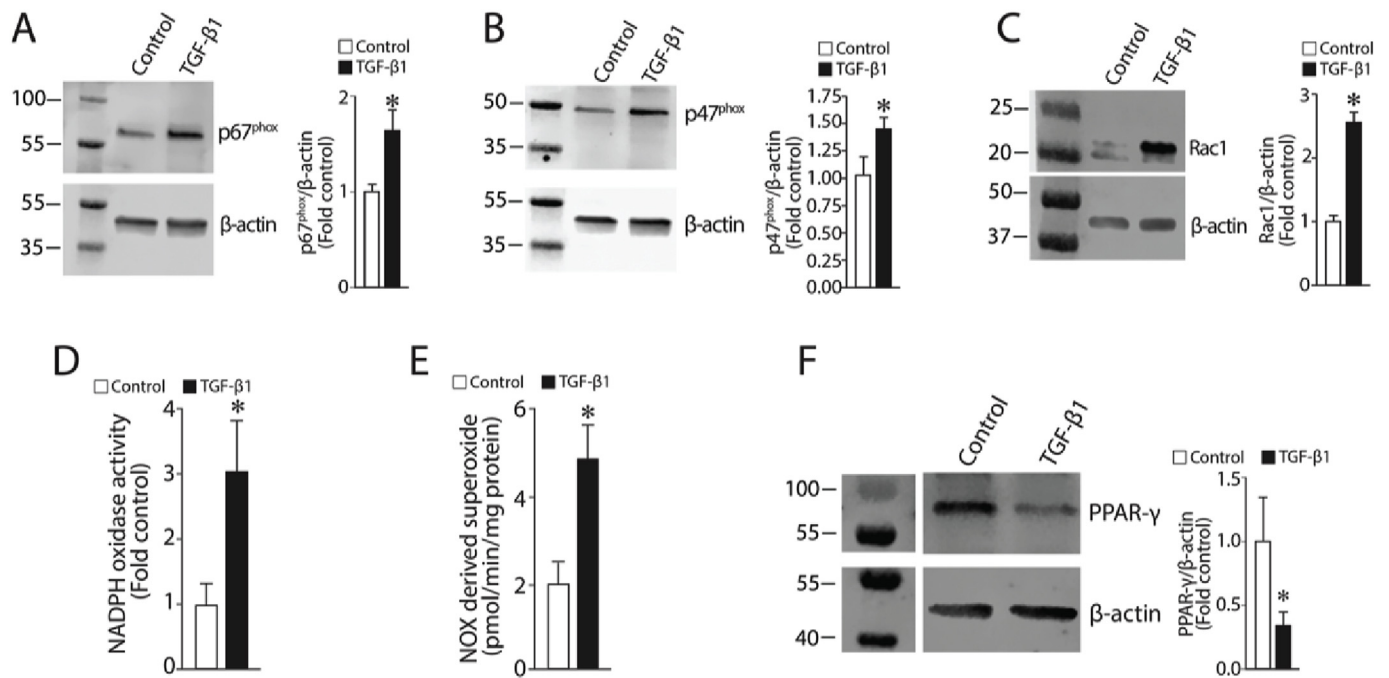


Fig. 5. TGF-β1 increases NADPH oxidase activity in pulmonary arterial endothelial cells. Western blot analyses indicate that TGF-β1 (5 ng/ml, 8 h) increases p67^{phox} (A), p47^{phox} (B) and Rac1 (C) protein levels. NOX activity (D) and NOX-derived superoxide (E) are also increased. However, PPAR-γ protein levels are decreased (F). Values are means ± SEM; n = 5–6. *P < 0.05 vs. untreated.

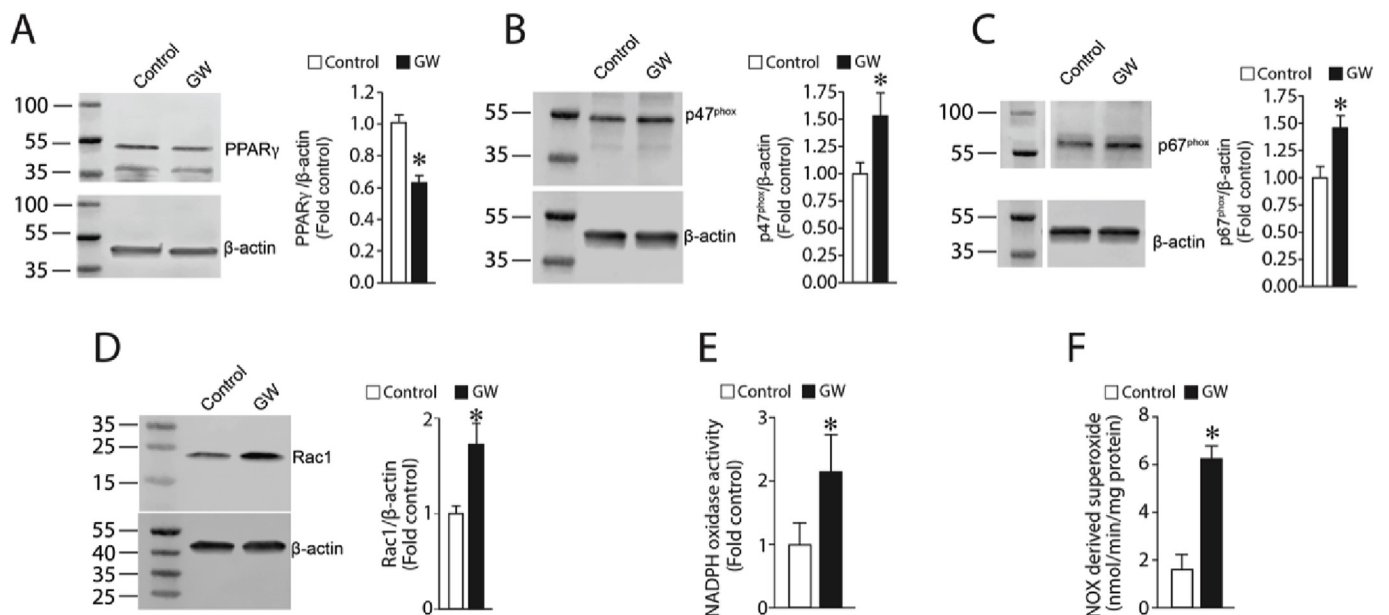


Fig. 6. The PPAR-γ antagonist GW9662 mimics the effects of TGF-β1 on NADPH oxidase activity in pulmonary arterial endothelial cells. Western blot analyses indicate that the PPAR-γ antagonist, GW9662 (5 μM, 24 h) decreases PPAR-γ protein levels (A) and increases p47^{phox} (B), p67^{phox} (C), and Rac1 (D) protein levels. NOX activity (E) and NOX-derived superoxide (F) also increase. Values are means ± SEM; n = 6. *P < 0.05 vs. untreated.

increases in mitochondrial ROS levels (Fig. 8C) and decrease in mitochondrial membrane potential (Fig. 8D). Mitochondrial bioenergetics was also disrupted as shown by significant decreases in maximal (Fig. 8E) and spare (Fig. 8F) respiratory capacities. Cellular ATP levels were also significantly attenuated (Fig. 8G) and this caused a reduction in eNOS-hsp90 interactions (Fig. 8H).

4. Discussion

TGF-β family members play important roles in vascular

development and vessel remodeling, and are critical in regulating macrophage, T cell, smooth muscle cell and endothelial cell signaling [2]. Dysregulated TGF-β signaling is associated with various chronic pulmonary diseases including asthma, chronic obstructive pulmonary disease, pulmonary fibrosis, and pulmonary vascular disease [1]. However, the mechanisms by which altered TGF-β signaling leads to pulmonary vascular disease are still incompletely understood. Our previous studies have shown that TGF-β1 expression is increased in a lamb model of PH that mimics congenital heart disease and increased PBF and pressure [7]. Our previous studies have also demonstrated that

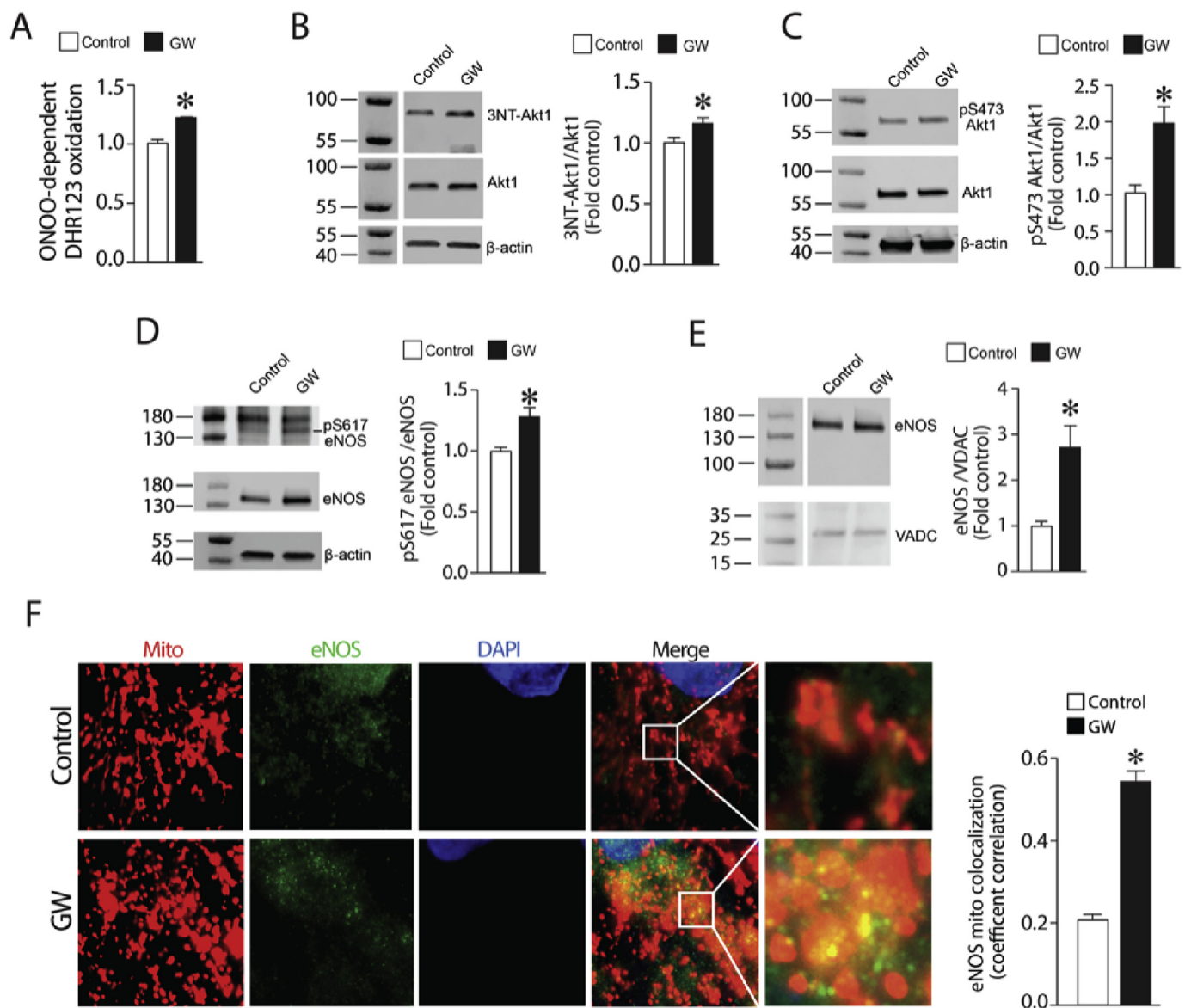


Fig. 7. GW9662 induces the mitochondrial redistribution of eNOS in pulmonary arterial endothelial cells. Treating PAEC with GW9662 (5 μ M, 24 h) increases peroxynitrite levels (A) and Akt1 nitration (B). Western blot analysis also shows that GW9662 significantly increases Akt1 activity, determined by increases in its phosphorylation at S473 (C) as well as the Akt1 mediated phosphorylation of eNOS at S617 (D). Western blot analysis of mitochondrial protein extracts (E) demonstrates that GW9662 increases eNOS mitochondrial redistribution. GW9662 also increases the mitochondrial levels of a GFP-tagged eNOS (F). The mitochondria are labeled with MitoTracker (red) and the extent of mitochondrial localization of eNOS was then determined by measuring the intensity of yellow fluorescence (overlap of red fluorescence of MitoTracker and green fluorescence of eNOS-GFP). Values are means \pm SEM; $n = 4-8$. * $P < 0.05$ vs. untreated. (For interpretation of the references to colour in this figure legend, the reader is referred to the Web version of this article.)

the disruption of mitochondrial bioenergetics plays a central role in the pulmonary vascular disease associated with CHD and increased PBF and pressure [27,29,30,36,37,42,52–55] and here we demonstrate that exposing PAEC to TGF- β 1 induces mitochondrial dysfunction and the disruption of mitochondrial bioenergetics. Further, we show that the loss of mitochondrial bioenergetics is caused, at least in part, by the disruption of carnitine homeostasis and fatty acid oxidation (FAO).

We have previously identified a reduction in FAO and carnitine homeostasis in both a lamb model [27,29,36,53] and in children born with complex congenital heart defects that result in increased PBF and pressure [30]. We have previously identified a reduction in FAO and carnitine homeostasis in both a lamb model [27,29,36,53] and in children born with complex congenital heart defects that result in increased PBF and pressure [30]. FAO produces acetyl-CoA to fuel the TCA cycle and reduces flavin adenine dinucleotide (FAD) and

nicotinamide adenine dinucleotide (NAD), for use in the electron transport chain [56–58]. Interestingly, recent studies from Finkels's group demonstrated that FAO, by regulating cellular acetyl-CoA levels, plays an important role in endothelial-mesenchymal transition (EndoMT) [59,60] causing ECs to develop fibroblast-like characteristics such as loss of cell-cell contacts, barrier dysfunction, and increased migratory potential [60]. EndoMT is now being recognized as an important player in the development of PH [61–63] and is stimulated by TGF- β 1 [59,64,65]. As TGF- β 1 signaling is increased, and FAO is disrupted, in models of PH it is interesting to speculate that the loss of FAO is a key driver of EndoMT in PH although further studies will be required to test this hypothesis.

Our data also demonstrate that the inhibition of carnitine homeostasis associated with TGF- β 1 exposure inhibits Complex I activity in PAEC. As Complex I is a major source of ROS in the mitochondria this

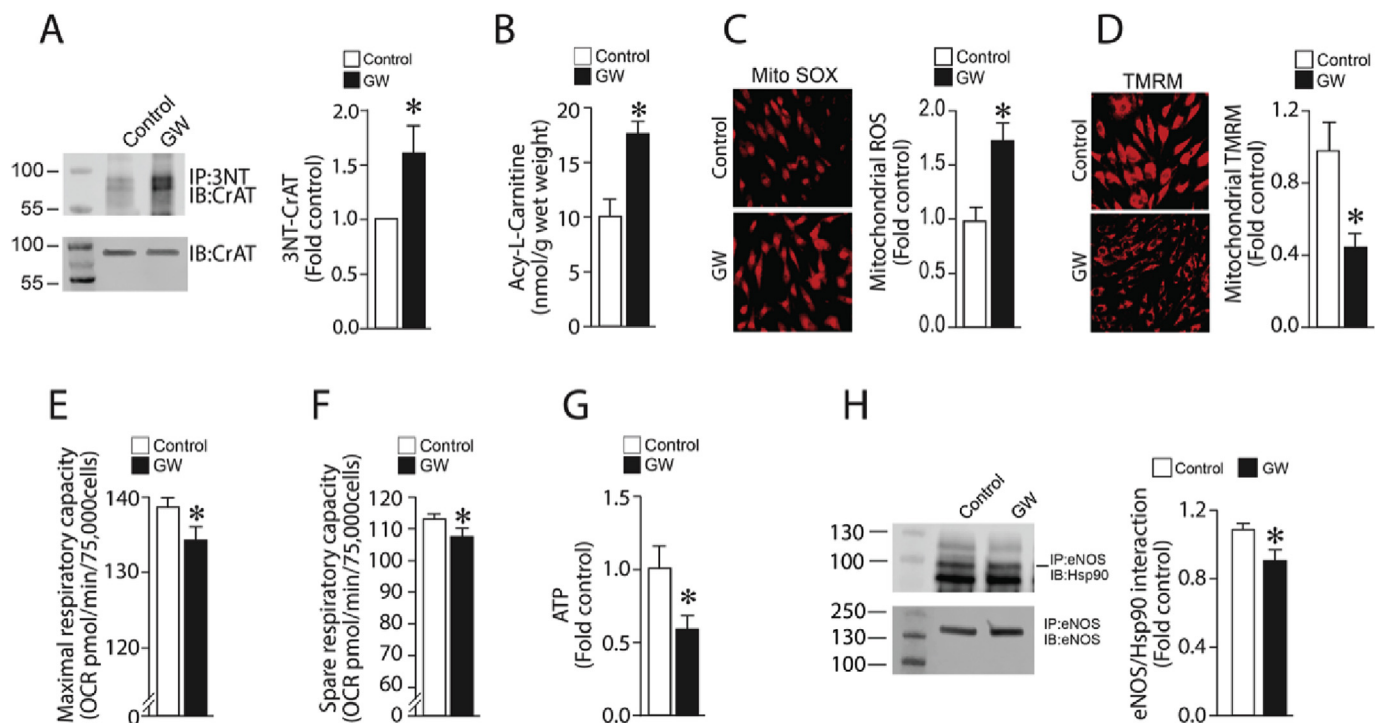


Fig. 8. GW9662 induces mitochondrial dysfunction and disrupts hsp90 activity in pulmonary arterial endothelial cells. GW9662 treatment (5 μ M, 24 h) significantly increased CrAT nitration levels (A) and increased acyl-L-carnitine levels (B). GW9662 also increases mitochondrial reactive oxygen species (ROS) generation in PAEC (C) and reduces the mitochondrial membrane potential (D). TGF- β 1 also affects mitochondrial bioenergetics as determined by significant reductions in the maximal respiratory capacity (E) and the spare respiratory capacity (F). Cellular ATP levels are decreased (G) and IP analysis demonstrated a reduction in eNOS-hsp90 interactions (H). Membranes were re-probed with hsp90 to normalize for IP efficiency. Values are means \pm SEM; n = 6 (A&B). n = 22–24 (C-F). n = n = 6–8 (G&H). *P < 0.05 vs. untreated.

likely represents the source of the increase in ROS we detected in TGF- β 1 exposed PAEC. In cells carnitine is found as either free carnitine (non-esterified molecule; FC), or acyl carnitines (esterified form; AC). A low AC/FC ratio is indicative of healthy mitochondria whereas a high AC/FC ratio suggests a decreased mitochondrial capacity for energy production. Carnitine and its derivatives are involved in the mitochondrial transport of fatty acids and are critical for the cell to maintain normal mitochondrial function. It is well established that the disruption of carnitine metabolism leads to mitochondrial dysfunction in cells. We have linked the loss of mitochondrial function to decreases in NO signaling. This occurs via a reduction in the ability of hsp90, an ATP-dependent chaperone, to interact with eNOS and GCH1, the rate limiting enzyme in the synthesis of the important NOS co-factor, BH₄ [28,55]. This results in the proteasomal degradation of GCH1 [28,33,55] and eNOS uncoupling. We have also identified important roles for increased expression of hsp70 as well as the E3 ubiquitin ligase, C-terminus of Hsp70-interacting protein, CHIP [28,33,55] in this process. The data in this study add to this knowledge by linking increased TGF- β 1 signaling to the loss of NO signaling in children born with congenital heart defects that result in increased PBF and pressure [30]. However, it should be noted that the effects of TGF- β 1 on eNOS are complex. For example, TGF- β 1 has been shown to increase eNOS expression in EC [66] and myocytes exposed to hypoxia-reoxygenation [67]. However, blocking TGF- β 1 signaling has also been shown to restore NO signaling in the nephropathy associated with cyclosporin A exposure in the mouse [68] and we have shown that increases in TGF- β 1 correlates with reductions in NO signaling [69,70]. Further, our data indicate that adding TGF- β 1 alone to PAEC did not significantly reduce basal NO levels but did attenuate shear mediated activation of eNOS. This suggests that TGF- β 1 may attenuate the activation of eNOS rather than basal NO generation perhaps through the reduction in hsp90 we have observed. However, further studies will be required to confirm this

possibility.

One of the effects of the disruption of mitochondrial bioenergetics by TGF- β 1 or GW9662 is an increase in mitochondrial derived reactive oxygen species (mt-ROS). There is a lot of interest in the role of mt-ROS both as signaling molecules and in pathologic outcomes. For example, we have previously shown that increases in mt-ROS can activate HIF-1 signaling even under normoxic conditions and that this can lead to metabolic reprogramming in cells to favor glycolysis and the development of a hyper-proliferative anti-apoptotic phenotype [37]. Conversely, increases in mt-ROS have been shown to be intimately involved in the EC apoptosis associated with ischemia/reperfusion (I/R) injury [71] and as an intermediate through which G Protein-Coupled Receptor mediated increases in intracellular Ca²⁺ can activate proinflammatory signaling and lead to increased leukocyte/EC adhesion [72] likely through the oxidation of the Mitochondrial Ca²⁺ Uniporter (MCU) [73]. Thus, it is interesting to speculate that mt-ROS could be involved some of the known effects of TGF- β 1 on EC function. For example, the EndoMT induced by long-term exposure of EC to TGF- β 1 [74,75] could require increases in mt-ROS. This possibility is strengthened by the fact that we recently demonstrated that EndoMT requires the activity of HIF-2 [75] and mt-ROS are known to stimulate HIF signaling [76–79]. However, possible links between mt-ROS and downstream events such as EndoMT are beyond the scope of the current study and will require future investigations.

Besides its normal caveolar location, eNOS can be targeted to the mitochondrion through the mitochondrial targeting loop located within aa627-631 (RRKRK) [80]. Our group was the first to show that the mitochondrial redistribution of eNOS [33,36,49,54] results in the disruption of mitochondrial bioenergetics [27,28,36,54]. Our data indicate that the disruption of mitochondrial bioenergetics induced by TGF- β 1 requires the mitochondrial redistribution of eNOS. A number of post translational modifications (PTMs) that are associated with the

mitochondrial redistribution of eNOS in our Shunt model of increased PBF and pressure. These include Akt1 nitration and phosphorylation [33,70] as well as the Akt1-mediated phosphorylation of eNOS at S617 [33,49]. However, the mechanism by which eNOS redistribution is regulated is still unresolved. Studies from Konduri's group have implicated hsp90 mediated binding to porin on the outer mitochondrial membrane as being involved in the redistribution of eNOS [81]. However, this is hard to integrate with our data indicating that hsp90 activity, at least measured by its ability to interact with eNOS, appears to be attenuated when PAEC are exposed to TGF- β 1. However, it is possible that there may be multiple pathways that can stimulate the mitochondrial redistribution of eNOS. For example, we have shown that eNOS can be redistributed to the mitochondria when it is phosphorylated at T495 and this occurs in the absence of changes in ATP [37] suggesting that hsp90 could be the responsible factor in this scenario. It is also possible that the mitochondrial redistribution of eNOS involves the binding of protein(s) to the eNOS mitochondrial translocation loop [49,80]. One such protein could be the molecular chaperone, CHIP. Although this possibility will have to be validated, CHIP is an attractive candidate as molecular chaperones are known to regulate the translocation of nuclear-encoded proteins into the mitochondrion [82,83]. In addition, its association with CHIP changes the sub-cellular distribution of eNOS [84], CHIP activity is stimulated by nitrosative stress [55], and CHIP is recruited to hsp90 chaperoned proteins [28]. Finally, CHIP contains a highly negatively charged region (¹⁸⁵EGDEDD1⁹⁰) [85], a sequence that could potentially interact with the positively charged eNOS mitochondrial targeting loop [49,80]. Our data also indicate that the nitration of Akt1 required to stimulate the phosphorylation of eNOS at S617 required to initiate the mitochondrial redistribution of eNOS [33,49] appears to require the activity of NOX and that the increase in NOX occurs secondary to the loss of peroxisome proliferator-activated receptor- γ (PPAR- γ) a member of the nuclear hormone receptor superfamily of ligand-activated transcription factors that are involved in the regulation of lipid and glucose metabolism [86–88]. In ECs there are a number of studies that indicate that PPAR- γ is an important regulator of NOX activity and NOX superoxide generation [89–92]. In our Shunt lamb model, we have shown that increased NOX derived superoxide correlates with decreased PPAR- γ activity [93] and that attenuating PPAR- γ activity is sufficient to disrupt mitochondrial function and induce pulmonary vascular disease in the neonatal lamb [52]. The data we present here adds to our knowledge by demonstrating that PPAR- γ inhibition in PAEC is sufficient to disrupt carnitine homeostasis and mitochondrial bioenergetics. The mechanism by which this occurs is likely through SMAD signaling as prior studies in human fetal fibroblasts have shown that a SMAD3-SMAD4 complex binds both to canonical SMAD-binding elements (SBEs) within the PPAR- γ promoter and a consensus TGF- β inhibitory element (TIE) resulting in the attenuation of promoter activity [94]. Conversely, PPAR- γ has been shown to attenuate Smad-dependent transcription of the COL1A2 gene [95] suggesting that there is a coregulation between PPAR- γ and Smad signaling that may be important for the development of endothelial dysfunction and the development of pulmonary vascular disease. Consistent with our data, TGF- β 1 reduces PPAR- γ expression in fibroblasts and hepatic stellate cells [96,97], although it does stimulate PPAR- γ expression in monocytes and macrophages [96,97] suggesting there may be cell specific events that could be explained by the presence or absence of eNOS.

In conclusion our data demonstrate that TGF- β signaling can attenuate mitochondrial function through the mitochondrial redistribution of eNOS and the disruption of carnitine homeostasis. This new mechanism of TGF- β signaling could be leveraged to develop new drug targets that could alleviate clinical conditions in which aberrant TGF- β signaling is known to play an important role.

Declaration of competing interest

The authors have no conflict of interest to declare related to the work contained in this submission.

Acknowledgements

This research was supported in part by HL60190 (SMB), HL137282 (SMB/JRF), HL134610 (SMB), HL142212 (SMB/EZ), and HL061284 (JRF) all from the National Institutes of Health.

Appendix A. Supplementary data

Supplementary data to this article can be found online at <https://doi.org/10.1016/j.redox.2020.101593>.

References

- [1] Y. Aschner, G.P. Downey, Transforming growth factor-beta: master regulator of the respiratory system in Health and disease, *Am. J. Respir. Cell Mol. Biol.* 54 (5) (2016) 647–655.
- [2] A. Bobik, Transforming growth factor-betas and vascular disorders, *Arterioscler. Thromb. Vasc. Biol.* 26 (8) (2006) 1712–1720.
- [3] N. Rol, K.B. Kurakula, C. Happe, H.J. Bogaard, M.J. Goumans, TGF-beta and BMP2 signaling in PAH: two black sheep in one family, *Int. J. Mol. Sci.* 19 (9) (2018).
- [4] M.D. Botney, L. Bahadori, L.I. Gold, Vascular remodeling in primary pulmonary hypertension. Potential role for transforming growth factor-beta, *Am. J. Pathol.* 144 (2) (1994) 286–295.
- [5] W. Ma, W. Han, P.A. Greer, R.M. Tuder, H.A. Toque, K.K. Wang, R.W. Caldwell, Y. Su, Calpain mediates pulmonary vascular remodeling in rodent models of pulmonary hypertension, and its inhibition attenuates pathologic features of disease, *J. Clin. Invest.* 121 (11) (2011) 4548–4566.
- [6] D. Jonigk, H. Golpon, C.L. Bockmeyer, L. Maegel, M.M. Hoepfer, J. Gottlieb, N. Nickel, K. Hussein, U. Maus, U. Lehmann, S. Janciauskiene, T. Welte, A. Haverich, J. Rische, H. Kreipe, F. Laenger, Plexiform lesions in pulmonary arterial hypertension composition, architecture, and microenvironment, *Am. J. Pathol.* 179 (1) (2011) 167–179.
- [7] E. Mata-Greenwood, B. Meyrick, R.H. Steinhorn, J.R. Fineman, S.M. Black, Alterations in TGF-beta1 expression in lambs with increased pulmonary blood flow and pulmonary hypertension, *Am. J. Physiol. Lung Cell Mol. Physiol.* 285 (1) (2003) L209–L221.
- [8] J.I. Hoffman, A.M. Rudolph, M.A. Heymann, Pulmonary vascular disease with congenital heart lesions: pathologic features and causes, *Circulation* 64 (5) (1981) 873–877.
- [9] B. Meyrick, L. Reid, Ultrastructural findings in lung biopsy material from children with congenital heart defects, *Am. J. Pathol.* 101 (3) (1980) 527–542.
- [10] M. Rabinovitch, S.G. Haworth, A.R. Castaneda, A.S. Nadas, L.M. Reid, Lung biopsy in congenital heart disease: a morphometric approach to pulmonary vascular disease, *Circulation* 58 (6) (1978) 1107–1122.
- [11] L.M. Reid, Structure and function in pulmonary hypertension, *New perceptions*, *Chest* 89 (2) (1986) 279–288.
- [12] L.M. Reid, The pulmonary circulation: remodeling in growth and disease. The 1978 J. Burns Amberson lecture, *Am. Rev. Respir. Dis.* 119 (4) (1979) 531–546.
- [13] M. Rabinovitch, J.F. Keane, W.I. Norwood, A.R. Castaneda, L. Reid, Vascular structure in lung tissue obtained at biopsy correlated with pulmonary hemodynamic findings after repair of congenital heart defects, *Circulation* 69 (4) (1984) 655–667.
- [14] S.G. Haworth, L. Reid, Quantitative structural study of pulmonary circulation in the newborn with aortic atresia, stenosis, or coarctation, *Thorax* 32 (2) (1977) 121–128.
- [15] S.G. Haworth, Pulmonary vascular disease in different types of congenital heart disease. Implications for interpretation of lung biopsy findings in early childhood, *Br. Heart J.* 52 (5) (1984) 557–571.
- [16] A. Hislop, S.G. Haworth, E.A. Shinebourne, L. Reid, Quantitative structural analysis of pulmonary vessels in isolated ventricular septal defect in infancy, *Br. Heart J.* 37 (10) (1975) 1014–1021.
- [17] D. Heath, J.E. Edwards, The pathology of hypertensive pulmonary vascular disease; a description of six grades of structural changes in the pulmonary arteries with special reference to congenital cardiac septal defects, *Circulation* 18 (4) (1958) 533–547.
- [18] N.T. Kouchoukos, E.H. Blackstone, J.W. Kirklin, Surgical implications of pulmonary hypertension in congenital heart disease, *Adv. Cardiol.* (22) (1978) 225–231.
- [19] M. Rabinovitch, T. Bothwell, B.N. Hayakawa, W.G. Williams, G.A. Trusler, R.D. Rowe, P.M. Olley, E. Cutz, Pulmonary artery endothelial abnormalities in patients with congenital heart defects and pulmonary hypertension. A correlation of light with scanning electron microscopy and transmission electron microscopy, *Lab. Invest.* 55 (6) (1986) 632–653.
- [20] D.S. Celermajer, S. Cullen, J.E. Deanfield, Impairment of endothelium-dependent pulmonary artery relaxation in children with congenital heart disease and abnormal pulmonary hemodynamics, *Circulation* 87 (2) (1993) 440–446.
- [21] A.T. Dinh-Xuan, Endothelial modulation of pulmonary vascular tone, *Eur. Respir. J.*

- 5 (6) (1992) 757–762.
- [22] F.A. Burrows, J.R. Klinck, M. Rabinovitch, D.J. Bohn, Pulmonary hypertension in children: perioperative management, *Can. Anaesth. Soc. J.* 33 (5) (1986) 606–628.
- [23] J. Wheller, B.L. George, D.G. Mulder, J.M. Jarmakani, Diagnosis and management of postoperative pulmonary hypertensive crisis, *Circulation* 60 (7) (1979) 1640–1644.
- [24] K.A. Hallidie-Smith, A. Hollman, W.P. Cleland, H.H. Bentall, J.F. Goodwin, Effects of surgical closure of ventricular septal defects upon pulmonary vascular disease, *Br. Heart J.* 31 (2) (1969) 246–260.
- [25] A. Szewczyk, W. Jarmuszkiwicz, A. Koziel, I. Sobieraj, W. Nobik, A. Lukasiak, A. Skup, P. Bednarczyk, B. Drabarek, D. Dymkowska, A. Wrzosek, K. Zablocki, Mitochondrial mechanisms of endothelial dysfunction, *Pharmacol. Rep.* 67 (4) (2015) 704–710.
- [26] Y. Mikhed, A. Daiber, S. Steven, Mitochondrial oxidative stress, mitochondrial DNA damage and their role in age-related vascular dysfunction, *Int. J. Mol. Sci.* 16 (7) (2015) 15918–15953.
- [27] S. Sharma, N. Sud, D.A. Wiseman, A.L. Carter, S. Kumar, Y. Hou, T. Rau, J. Wilham, C. Harmon, P. Oishi, J.R. Fineman, S.M. Black, Altered carnitine homeostasis is associated with decreased mitochondrial function and altered nitric oxide signaling in lambs with pulmonary hypertension, *Am. J. Physiol. Lung Cell Mol. Physiol.* 294 (1) (2008) L46–L56.
- [28] S. Sharma, X. Sun, S. Kumar, R. Rafikov, A. Aramburo, G. Kalkan, J. Tian, I. Rehmani, S. Kallarackal, J.R. Fineman, S.M. Black, Preserving mitochondrial function prevents the proteasomal degradation of GTP cyclohydrolase I, *Free Radic. Biol. Med.* 53 (2) (2012) 216–229.
- [29] S. Sharma, X. Sun, R. Rafikov, S. Kumar, Y. Hou, P.E. Oishi, S.A. Datar, G. Raff, J.R. Fineman, S.M. Black, PPAR-gamma regulates carnitine homeostasis and mitochondrial function in a lamb model of increased pulmonary blood flow, *PLoS One* 7 (9) (2012) e41555.
- [30] S.M. Black, A. Field-Ridley, S. Sharma, S. Kumar, R.L. Keller, R. Kameny, E. Maltepe, S.A. Datar, J.R. Fineman, Altered carnitine homeostasis in children with increased pulmonary blood flow due to ventricular septal defects, *Pediatr. Crit. Care Med.* 18 (10) (2017) 931–934.
- [31] R. Mathew, Pulmonary hypertension and metabolic syndrome: possible connection, PPARgamma and Caveolin-1, *World J. Cardiol.* 6 (8) (2014) 692–705.
- [32] R.E. Nisbet, R.L. Sutliff, C.M. Hart, The role of peroxisome proliferator-activated receptors in pulmonary vascular disease, *PPAR Res.* 2007 (2007) 18797.
- [33] X. Sun, M. Kellner, A.A. Desai, T. Wang, Q. Lu, A. Kangath, N. Qu, C. Klingner, S. Fratz, J.X. Yuan, J.R. Jacobson, J.G. Garcia, R. Rafikov, J.R. Fineman, S.M. Black, Asymmetric dimethylarginine stimulates Akt1 phosphorylation via heat shock protein 70-facilitated carboxyl-terminal modulator protein degradation in pulmonary arterial endothelial cells, *Am. J. Respir. Cell Mol. Biol.* 55 (2) (2016) 275–287.
- [34] L.K. Kelly, S. Wedgwood, R.H. Steinhorn, S.M. Black, Nitric oxide decreases endothelin-1 secretion through the activation of soluble guanylate cyclase, *Am. J. Physiol. Lung Cell Mol. Physiol.* 286 (5) (2004) L984–L991.
- [35] X. Sun, S. Fratz, S. Sharma, Y. Hou, R. Rafikov, S. Kumar, I. Rehmani, J. Tian, A. Smith, C. Schreiber, J. Reiser, S. Naumann, S. Haag, J. Hess, J.D. Catravas, C. Patterson, J.R. Fineman, S.M. Black, CHIP-dependent GTP cyclohydrolase I degradation in lambs with increased pulmonary blood flow, *Am. J. Respir. Cell Mol. Biol.*
- [36] X. Sun, S. Sharma, S. Fratz, S. Kumar, R. Rafikov, S. Aggarwal, O. Rafikova, Q. Lu, T. Burns, S. Dasarathy, J. Wright, C. Schreiber, M. Radman, J.R. Fineman, S.M. Black, Disruption of endothelial cell mitochondrial bioenergetics in lambs with increased pulmonary blood flow, *Antioxidants Redox Signal.* 18 (14) (2013) 1739–1752.
- [37] X. Sun, S. Kumar, S. Sharma, S. Aggarwal, Q. Lu, C. Gross, O. Rafikova, S.G. Lee, S. Dasarathy, Y. Hou, M.L. Meadows, W. Han, Y. Su, J.R. Fineman, S.M. Black, Endothelin-1 induces a glycolytic switch in pulmonary arterial endothelial cells via the mitochondrial translocation of endothelial nitric oxide synthase, *Am. J. Respir. Cell Mol. Biol.* 50 (6) (2014) 1084–1095.
- [38] N. Sud, S. Sharma, D.A. Wiseman, C. Harmon, S. Kumar, R.C. Venema, J.R. Fineman, S.M. Black, Nitric oxide and superoxide generation from endothelial NOS: modulation by HSP90, *Am. J. Physiol. Lung Cell Mol. Physiol.* 293 (6) (2007) L1444–L1453.
- [39] Q. Lu, M.S. Wainwright, V.A. Harris, S. Aggarwal, Y. Hou, T. Rau, D.J. Poulsen, S.M. Black, Increased NADPH oxidase-derived superoxide is involved in the neuronal cell death induced by hypoxia-ischemia in neonatal hippocampal slice cultures, *Free Radic. Biol. Med.* 53 (5) (2012) 1139–1151.
- [40] S. Kumar, N. Sud, F.V. Fonseca, Y. Hou, S.M. Black, Shear stress stimulates nitric oxide signaling in pulmonary arterial endothelial cells via a reduction in catalase activity: role of protein kinase C delta, *Am. J. Physiol. Lung Cell Mol. Physiol.* 298 (1) (2010) L105–L116.
- [41] B.T. Tang, S.S. Pickard, F.P. Chan, P.S. Tsao, C.A. Taylor, J.A. Feinstein, Wall shear stress is decreased in the pulmonary arteries of patients with pulmonary arterial hypertension: an image-based, computational fluid dynamics study, *Pulm. Circ.* 2 (4) (2012) 470–476.
- [42] S. Sharma, X. Sun, S. Agarwal, R. Rafikov, S. Dasarathy, S. Kumar, S.M. Black, Role of carnitine acetyl transferase in regulation of nitric oxide signaling in pulmonary arterial endothelial cells, *Int. J. Mol. Sci.* 14 (1) (2012) 255–272.
- [43] S. Kumar, P.E. Oishi, R. Rafikov, S. Aggarwal, Y. Hou, S.A. Datar, S. Sharma, A. Azakie, J.R. Fineman, S.M. Black, Tezosentan increases nitric oxide signaling via enhanced hydrogen peroxide generation in lambs with surgically induced acute increases in pulmonary blood flow, *J. Cell. Biochem.* 114 (2) (2013) 435–447.
- [44] J. Tian, Y. Hou, Q. Lu, D.A. Wiseman, F. Vasconcelos Fonseca, S. Elms, D.J. Fulton, S.M. Black, A novel role for caveolin-1 in regulating endothelial nitric oxide synthase activation in response to H2O2 and shear stress, *Free Radic. Biol. Med.* 49 (2) (2010) 159–170.
- [45] S. Bolte, F.P. Cordelieres, A guided tour into subcellular colocalization analysis in light microscopy, *J. Microsc.* 224 (Pt 3) (2006) 213–232.
- [46] S. Aggarwal, C.M. Gross, S. Kumar, S. Datar, P. Oishi, G. Kalkan, C. Schreiber, S. Fratz, J.R. Fineman, S.M. Black, Attenuated vasodilatation in lambs with endogenous and exogenous activation of cGMP signaling: role of protein kinase G nitration, *J. Cell. Physiol.* 226 (12) (2011) 3104–3113.
- [47] R. Rafikov, X. Sun, O. Rafikova, M. Louise Meadows, A.A. Desai, Z. Khalpey, J.X. Yuan, J.R. Fineman, S.M. Black, Complex I dysfunction underlies the glycolytic switch in pulmonary hypertensive smooth muscle cells, *Redox Biol* 6 (2015) 278–286.
- [48] M.D. Brand, D.G. Nicholls, Assessing mitochondrial dysfunction in cells, *Biochem. J.* 435 (2) (2011) 297–312.
- [49] R. Rafikov, O. Rafikova, S. Aggarwal, C. Gross, X. Sun, J. Desai, D. Fulton, S.M. Black, Asymmetric dimethylarginine induces endothelial nitric-oxide synthase mitochondrial redistribution through the nitration-mediated activation of Akt1, *J. Biol. Chem.* 288 (9) (2013) 6212–6226.
- [50] M. Kellner, S. Noonepalle, Q. Lu, A. Srivastava, E. Zemskov, S.M. Black, ROS signaling in the pathogenesis of acute lung injury (ALI) and acute respiratory distress syndrome (ARDS), *Adv. Exp. Med. Biol.* 967 (2017) 105–137.
- [51] E. Mata-Greenwood, A. Grobe, S. Kumar, Y. Noskina, S.M. Black, Cyclic stretch increases VEGF expression in pulmonary arterial smooth muscle cells via TGF-beta1 and reactive oxygen species: a requirement for NAD(P)H oxidase, *Am. J. Physiol. Lung Cell Mol. Physiol.* 289 (2) (2005) L288–L289.
- [52] S. Sharma, J. Barton, R. Rafikov, S. Aggarwal, H.C. Kuo, P.E. Oishi, S.A. Datar, J.R. Fineman, S.M. Black, Chronic inhibition of PPAR-gamma signaling induces endothelial dysfunction in the juvenile lamb, *Pulm. Pharmacol. Therapeut.* 26 (2) (2013) 271–280.
- [53] S. Sharma, A. Aramburo, R. Rafikov, X. Sun, S. Kumar, P.E. Oishi, S.A. Datar, G. Raff, K. Xoinis, G. Kalkan, S. Fratz, J.R. Fineman, S.M. Black, L-carnitine preserves endothelial function in a lamb model of increased pulmonary blood flow, *Pediatr. Res.* 74 (1) (2013) 39–47.
- [54] N. Sud, S.M. Wells, S. Sharma, D.A. Wiseman, J. Wilham, S.M. Black, Asymmetric dimethylarginine inhibits HSP90 activity in pulmonary arterial endothelial cells: role of mitochondrial dysfunction, *Am. J. Physiol. Cell Physiol.* 294 (6) (2008) C1407–C1418.
- [55] X. Sun, S. Fratz, S. Sharma, Y. Hou, R. Rafikov, S. Kumar, I. Rehmani, J. Tian, A. Smith, C. Schreiber, J. Reiser, S. Naumann, S. Haag, J. Hess, J.D. Catravas, C. Patterson, J.R. Fineman, S.M. Black, C-terminus of heat shock protein 70-interacting protein-dependent GTP cyclohydrolase I degradation in lambs with increased pulmonary blood flow, *Am. J. Respir. Cell Mol. Biol.* 45 (1) (2011) 163–171.
- [56] A.M. Lundsgaard, A.M. Fritzen, B. Kiens, Molecular regulation of fatty acid oxidation in skeletal muscle during aerobic exercise, *Trends Endocrinol. Metabol.* 29 (1) (2018) 18–30.
- [57] M.M. Adeva-Andany, N. Carneiro-Freire, M. Seco-Filgueira, C. Fernandez-Fernandez, D. Mourino-Bayolo, Mitochondrial beta-oxidation of saturated fatty acids in humans, *Mitochondrion* 46 (2019) 73–90.
- [58] S. Eaton, Control of mitochondrial beta-oxidation flux, *Prog. Lipid Res.* 41 (3) (2002) 197–239.
- [59] J. Xiong, H. Kawagishi, Y. Yan, J. Liu, Q.S. Wells, L.R. Edmunds, M.M. Fergusson, Z.X. Yu, Rovira II, E.L. Brittain, M.J. Wolfgang, M.J. Jurczak, J.P. Fessel, T. Finkel, A metabolic basis for endothelial-to-mesenchymal transition, *Mol. Cell* 69 (4) (2018) 689–698 e7.
- [60] P. Strzyz, Metabolism: a metabolic switch of fate, *Nat. Rev. Mol. Cell Biol.* 19 (4) (2018) 211.
- [61] R.B. Good, A.J. Gilbane, S.L. Trinder, C.P. Denton, G. Coghlan, D.J. Abraham, A.M. Holmes, Endothelial to mesenchymal transition contributes to endothelial dysfunction in pulmonary arterial hypertension, *Am. J. Pathol.* 185 (7) (2015) 1850–1858.
- [62] B. Ranchoux, F. Antigny, C. Rucker-Martin, A. Hautefort, C. Pechoux, H.J. Bogaard, P. Dorfmuller, S. Remy, F. Lecker, S. Plante, S. Chat, E. Fadel, A. Houssaini, I. Anegon, S. Adnot, G. Simonneau, M. Humbert, S. Cohen-Kaminsky, F. Perros, Endothelial-to-mesenchymal transition in pulmonary hypertension, *Circulation* 131 (11) (2015) 1006–1018.
- [63] X. Lu, J. Gong, P.A. Denery, H. Yao, Endothelial-to-mesenchymal transition: pathogenesis and therapeutic targets for chronic pulmonary and vascular diseases, *Biochem. Pharmacol.* 168 (2019) 100–107.
- [64] S. Song, M. Zhang, Z. Yi, H. Zhang, T. Shen, X. Yu, C. Zhang, X. Zheng, L. Yu, C. Ma, Y. Liu, D. Zhu, The role of PDGF-B/TGF-beta1/neprilysin network in regulating endothelial-to-mesenchymal transition in pulmonary artery remodeling, *Cell. Signal.* 28 (10) (2016) 1489–1501.
- [65] P.J. Wermuth, Z. Li, F.A. Mendoza, S.A. Jimenez, Stimulation of transforming growth factor-beta1-induced endothelial-to-mesenchymal transition and tissue fibrosis by endothelin-1 (ET-1): a novel profibrotic effect of ET-1, *PLoS One* 11 (9) (2016) e0161988.
- [66] N. Inoue, R.C. Venema, H.S. Sayegh, Y. Ohara, T.J. Murphy, D.G. H. Molecular regulation of the bovine endothelial cell nitric oxide synthase by transforming growth factor-beta 1, *Arteriosclerosis, Thrombosis & Vascular Biology* 15 (1995) 1255–1261.
- [67] H. Chen, D. Li, T. Saldeen, J.L. Mehta, TGF-beta(1) modulates NOS expression and phosphorylation of Akt/PKB in rat myocytes exposed to hypoxia-reoxygenation, *Am. J. Physiol. Heart Circ. Physiol.* 281 (3) (2001) H1035–H1039.
- [68] H. Ling, X. Li, S. Jha, W. Wang, L. Karetskaya, B. Pratt, S. Ledbetter, Therapeutic role of TGF-beta-neutralizing antibody in mouse cyclosporin A nephropathy: morphologic improvement associated with functional preservation, *J. Am. Soc.*

- Nephrol. 14 (2) (2003) 377–388.
- [69] E. Mata-Greenwood, B. Meyrick, J.R. Fineman, S.M. Black, Alterations in TGF- β 1 expression in lambs with increased pulmonary blood flow and pulmonary hypertension, *Am. J. Physiol.* 285 (2003) L209–L221.
- [70] P.E. Oishi, D.A. Wiseman, S. Sharma, S. Kumar, Y. Hou, S.A. Datar, A. Azakie, M.J. Johengen, C. Harmon, S. Fratz, J.R. Fineman, S.M. Black, Progressive dysfunction of nitric oxide synthase in a lamb model of chronically increased pulmonary blood flow: a role for oxidative stress, *Am. J. Physiol. Lung Cell Mol. Physiol.* 295 (5) (2008) L756–L766.
- [71] M. Madesh, B.J. Hawkins, T. Milovanova, C.D. Bhanumathy, S.K. Joseph, S.P. Ramachandrarao, K. Sharma, T. Kurosaki, A.B. Fisher, Selective role for superoxide in InsP3 receptor-mediated mitochondrial dysfunction and endothelial apoptosis, *J. Cell Biol.* 170 (7) (2005) 1079–1090.
- [72] B.J. Hawkins, L.A. Solt, I. Chowdhury, A.S. Kazi, M.R. Abid, W.C. Aird, M.J. May, J.K. Foskett, M. Madesh, G protein-coupled receptor Ca $^{2+}$ -linked mitochondrial reactive oxygen species are essential for endothelial/leukocyte adherence, *Mol. Cell Biol.* 27 (21) (2007) 7582–7593.
- [73] Z. Dong, S. Shanmughapriya, D. Tomar, N. Siddiqui, S. Lynch, N. Nemani, S.L. Breves, X. Zhang, A. Tripathi, P. Palaniappan, M.F. Riitano, A.M. Worth, A. Seelam, E. Carvalho, R. Subbiah, F. Jana, J. Soboloff, Y. Peng, J.Y. Cheung, S.K. Joseph, J. Caplan, S. Rajan, P.B. Stathopoulos, M. Madesh, Mitochondrial Ca (2+) uniporter is a mitochondrial luminal redox sensor that augments MCU channel activity, *Mol. Cell* 65 (6) (2017) 1014–1028 e7.
- [74] P.J. Wermuth, K.R. Carney, F.A. Mendoza, S. Piera-Velazquez, S.A. Jimenez, Endothelial cell-specific activation of transforming growth factor- β signaling in mice induces cutaneous, visceral, and microvascular fibrosis, *Lab. Invest.* 97 (7) (2017) 806–818.
- [75] H. Tang, A. Babicheva, K.M. McDermott, Y. Gu, R.J. Ayon, S. Song, Z. Wang, A. Gupta, T. Zhou, X. Sun, S. Dash, Z. Wang, A. Balistrieri, Q. Zheng, A.G. Cordery, A.A. Desai, F. Rischard, Z. Khalpey, J. Wang, S.M. Black, J.G.N. Garcia, A. Makino, J.X. Yuan, Endothelial HIF-2 α contributes to severe pulmonary hypertension due to endothelial-to-mesenchymal transition, *Am. J. Physiol. Lung Cell Mol. Physiol.* 314 (2) (2018) L256–L275.
- [76] E. Belaidi, J. Morand, E. Gras, J.L. Pepin, D. Godin-Ribuot, Targeting the ROS-HIF-1-endothelin axis as a therapeutic approach for the treatment of obstructive sleep apnea-related cardiovascular complications, *Pharmacol. Ther.* 168 (2016) 1–11.
- [77] A.B. Hwang, S.J. Lee, Regulation of life span by mitochondrial respiration: the HIF-1 and ROS connection, *Aging (Albany NY)* 3 (3) (2011) 304–310.
- [78] A. Galanis, A. Pappa, A. Giannakakis, E. Lanitis, D. Dangaj, R. Sandaltzopoulos, Reactive oxygen species and HIF-1 signalling in cancer, *Canc. Lett.* 266 (1) (2008) 12–20.
- [79] N.R. Prabhakar, G.K. Kumar, J. Nanduri, Intermittent hypoxia-mediated plasticity of acute O $_2$ sensing requires altered red-ox regulation by HIF-1 and HIF-2, *Ann. N. Y. Acad. Sci.* 1177 (2009) 162–168.
- [80] S. Gao, J. Chen, S.V. Brodsky, H. Huang, S. Adler, J.H. Lee, N. Dhadwal, L. Cohen-Gould, S.S. Gross, M.S. Goligorsky, Docking of endothelial nitric oxide synthase (eNOS) to the mitochondrial outer membrane: a pentabasic amino acid sequence in the autoinhibitory domain of eNOS targets a proteinase K-cleavable peptide on the cytoplasmic face of mitochondria, *J. Biol. Chem.* 279 (16) (2004) 15968–15974.
- [81] G.G. Konduri, A.J. Afolayan, A. Eis, K.A. Pritchard Jr., R.J. Teng, Interaction of endothelial nitric oxide synthase with mitochondria regulates oxidative stress and function in fetal pulmonary artery endothelial cells, *Am. J. Physiol. Lung Cell Mol. Physiol.* 309 (9) (2015) L1009–L1017.
- [82] W. Neupert, Protein import into mitochondria, *Annu. Rev. Biochem.* 66 (1997) 863–917.
- [83] P.J. Kang, J. Ostermann, J. Shilling, W. Neupert, E.A. Craig, N. Pfanner, Requirement for hsp70 in the mitochondrial matrix for translocation and folding of precursor proteins, *Nature* 348 (6297) (1990) 137–143.
- [84] J. Jiang, D. Cyr, R.W. Babbitt, W.C. Sessa, C. Patterson, Chaperone-dependent regulation of endothelial nitric-oxide synthase intracellular trafficking by the co-chaperone/ubiquitin ligase CHIP, *J. Biol. Chem.* 278 (49) (2003) 49332–49341.
- [85] C.A. Ballinger, P. Connell, Y. Wu, Z. Hu, L.J. Thompson, L.Y. Yin, C. Patterson, Identification of CHIP, a novel tetratricopeptide repeat-containing protein that interacts with heat shock proteins and negatively regulates chaperone functions, *Mol. Cell Biol.* 19 (6) (1999) 4535–4545.
- [86] P. Corrales, A. Izquierdo-Lahuerta, G. Medina-Gomez, Maintenance of kidney metabolic homeostasis by PPAR gamma, *Int. J. Mol. Sci.* 19 (7) (2018).
- [87] C.M. Hart, The Role of PPARgamma in pulmonary vascular disease, *J. Invest. Med.* 56 (2) (2008) 518–521.
- [88] R.L. Sutliff, B.Y. Kang, C.M. Hart, PPARgamma as a potential therapeutic target in pulmonary hypertension, *Ther. Adv. Respir. Dis.* 4 (3) (2010) 143–160.
- [89] J. Hwang, D.J. Kleinhenz, B. Lassegue, K.K. Griendling, S. Dikalov, C.M. Hart, Peroxisome proliferator-activated receptor-gamma ligands regulate endothelial membrane superoxide production, *Am. J. Physiol. Cell Physiol.* 288 (4) (2005) C899–C905.
- [90] T.M. De Silva, Y. Li, D.A. Kinzenbaw, C.D. Sigmund, F.M. Faraci, Endothelial PPARgamma (peroxisome proliferator-activated receptor-gamma) is essential for preventing endothelial dysfunction with aging, *Hypertension* 72 (1) (2018) 227–234.
- [91] J.W. Xu, K. Ikeda, Y. Yamori, Genistein inhibits expressions of NADPH oxidase p22phox and angiotensin II type 1 receptor in aortic endothelial cells from stroke-prone spontaneously hypertensive rats, *Hypertens. Res.* 27 (9) (2004) 675–683.
- [92] M.C. Wagner, S.M. Yeligar, L.A. Brown, C. Michael Hart, PPARgamma ligands regulate NADPH oxidase, eNOS, and barrier function in the lung following chronic alcohol ingestion, *Alcohol Clin. Exp. Res.* 36 (2) (2012) 197–206.
- [93] P.E. Oishi, S. Sharma, S.A. Datar, S. Kumar, S. Aggarwal, Q. Lu, G. Raff, A. Azakie, J.H. Hsu, E. Sajti, S. Fratz, S.M. Black, J.R. Fineman, Rosiglitazone preserves pulmonary vascular function in lambs with increased pulmonary blood flow, *Pediatr. Res.* 73 (1) (2013) 54–61.
- [94] S.P. Lakshmi, A.T. Reddy, R.C. Reddy, Transforming growth factor beta suppresses peroxisome proliferator-activated receptor gamma expression via both SMAD binding and novel TGF- β inhibitory elements, *Biochem. J.* 474 (9) (2017) 1531–1546.
- [95] A.K. Ghosh, S. Bhattacharyya, J. Wei, S. Kim, Y. Barak, Y. Mori, J. Varga, Peroxisome proliferator-activated receptor-gamma abrogates Smad-dependent collagen stimulation by targeting the p300 transcriptional coactivator, *Faseb. J.* 23 (9) (2009) 2968–2977.
- [96] A.T. Dantas, M.C. Pereira, M.J. de Melo Rego, L.F. da Rocha Jr., R. Pitta Ida, C.D. Marques, A.L. Duarte, M.G. Pitta, The role of PPAR gamma in systemic sclerosis, *PPAR Res.* 2015 (2015) 124624.
- [97] J. Wei, S. Bhattacharyya, M. Jain, J. Varga, Regulation of matrix remodeling by peroxisome proliferator-activated receptor-gamma: a novel link between metabolism and fibrogenesis, *Open Rheumatol. J.* 6 (2012) 103–115.